Pergamon

J. Biomechanics, Vol. 28, No. 5, pp. 513–525, 1995

0021-9290/95 $9.50 + .00

0021-9290(94)00114-6

VARIATION OF MUSCLE MOMENT ARMS WITH ELBOW AND FOREARM POSITION

Wendy M. Murray, Scott L. Delp and Thomas S. Buchanan

Departments of Biomedical Engineering and Physical Medicine & Rehabilitation Northwestern University, and Sensory Motor Performance Program, Rehabilitation Institute of Chicago, 345 East Superior St., Chicago, IL 60611, U.S.A.

Abstract—We hypothesized that the moment arms of muscles crossing the elbow vary substantially with forearm and elbow position and that these variations could be represented using a three-dimensional computer model. Flexion/extension and pronation/supination moment arms of the brachioradialis, biceps, brachialis, pronator teres, and triceps were calculated from measurements of tendon displacement and joint angle in two anatomic specimens and were estimated using a computer model of the elbow joint. The anatomical measurements revealed that the flexion/extension moment arms varied by at least 30% over a 95° range of motion. The changes in flexion/extension moment arm magnitudes with elbow flexion angle were represented well by the computer model. The anatomical studies and the computer model demonstrate that the biceps flexion moment arm peaks in a more extended elbow position and has a larger peak when the forearm is supinated. Also, the peak biceps supination moment arm decreases as the elbow is extended. These results emphasize the need to account for the variation of muscle moment arms with elbow flexion and forearm position.

INTRODUCTION

Reliable estimates of muscle moment arms are necessary to calculate accurately the forces and moments generated by muscles. When muscle forces are calculated from experimental measurements of joint moments using optimization methods, muscle moment arms are coefficients in the equilibrium equations, and thus influence the results of the optimization (Herzog, 1992). Similarly, when musculoskeletal models are used to estimate joint moments based on muscle activations, the muscle moment arms transform the modeled muscle forces into joint moments. However, determining the muscle moment arms has often been considered to be an intermediate or unimportant step. In many studies, limited information on the method for estimation of muscle moment arms is reported (Dul *et al.*, 1984; Edgerton *et al.*, 1990) or the resulting moment arm values are not reported (Caldwell and Chapman, 1989; Seireg and Arvikar, 1973).

We hypothesized that the moment arms of muscles crossing the elbow joint vary substantially as a function of both elbow flexion angle and the forearm pronation/supination position. We further hypothesized that these variations could be represented in a three-dimensional computer model that accurately characterized the musculoskeletal geometry and the joint kinematics. Previous studies of elbow muscle moment arms have not fully investigated the variation of moment arms with elbow and forearm position. Amis *et al.* (1979) computed elbow flexion moment arms over a full range of flexion angles, but did not report pronation/supination moment arms, or the effect of forearm position on flexion/extension moment arms. Anatomical measurements of elbow muscle moment arms made in previous studies have not provided enough data to determine the variation of moment arms with elbow and forearm position (An *et al.*, 1981, 1984a; Crowninshield and Brand, 1981). In addition, a wide range of magnitudes of moment arms have been reported for the same elbow muscle, and the causes of these disparities remain unclear.

To determine the dependence of elbow muscle moment arms on elbow and forearm position, flexion/extension and pronation/supination moment arms of five major muscles were calculated from measurements of tendon displacement and joint angle in two cadaver specimens. In addition, a computer model of the elbow and surrounding muscles was developed to estimate moment arms over a range of elbow and forearm positions, and to examine the sensitivity of muscle moment arms to various representations of the musculoskeletal geometry.

METHODS

Flexion/extension and pronation/supination moment arms were calculated from measurements of tendon displacement and joint angle from the right arms of two alcohol-preserved cadavers (see Table 1 for the anthropometric data of each specimen). The limbs were disarticulated at the shoulder and the skin

Received in final form 27 *July* 1994.
Address correspondence to: Dr Thomas S. Buchanan, Sensory Motor Performance Program, Rehabilitation Institute of Chicago (1406), 345 E. Superior St, Chicago, IL 60611, U.S.A.

Table 1. Anthropometric data of the two specimen and the model*

	Male	Female	Model
Humerus length†	33.0	28.5	30.3
Radius length‡	24.0	21.0	22.3
Ulna length§	27.0	24.0	24.5
Transepicondylar width	6.7	6.0	6.1
Forearm width (just inferior to the radial head)	4.5	3.6	3.9
Anterior/posterior thickness at trochlear capitellar ridge	2.5	2.6	2.1
Age at death	90	82	—

*All dimensions are in centimeters.

†Measured from the top of the humeral head to the base of the trochlea.

‡Measured from the tip of the olecranon to the styloid process of the ulna.

§Measured from the head of the radius to the styloid process of the radius.

and fascia proximal to the elbow joint were removed; the tissue around the elbow was disturbed as little as possible. The long head of the biceps, the brachialis, the brachioradialis, the pronator teres, and the medial head of the triceps were studied.

Each muscle was prepared by releasing it from its origin and surrounding fascia, and removing a proximal part of the muscle. A nylon mesh was sewn to the muscle belly, and a wire was attached to the mesh. The muscle was connected to a Celesco PT101 position transducer (Celesco Transducer Products, Canoga Park, CA) by the wire. The transducer applies a constant tension of 7.5 N and the experimental setup was accurate to $\pm$ 0.027 mm.

Each muscle was constrained to follow its anatomical path. The anatomical constraint for the biceps muscle path was the intertubercular sulcus and the fascia surrounding it. The brachioradialis and pronator teres were routed through a hole drilled through the humerus at their respective origins. None of these constraints moved, because they were permanent parts of the anatomy of the specimen. A U-bolt was placed loosely around the humerus to maintain the brachialis anatomical path. The movement of the brachialis muscle was monitored throughout the anatomical measurements.

Tendon displacement vs elbow flexion angle was collected using the following method. A goniometer that ranged from 0 to 180° elbow flexion in 5° increments was etched onto the surface of a Plexiglas® sheet. The medial epicondyle of the humerus rested on the center point of the goniometer, and the humerus was kept stationary while the elbow was moved through its range of motion. Angle measurements were made by aligning a pointer attached to the wrist with the etchings in the Plexiglas® (Fig. 1A). When the elbow was extended, the forearm moved out of the horizontal plane due to the carrying angle, which is the angle formed by the long axis of the humerus and the long axis of the ulna in the frontal plane. In full extension, the carrying angle averages 10–15° degrees in men and 15–20° degrees in women (An and Morrey, 1985). To account for this, the pointer was contained within a cylinder that allowed the vertical position of the pointer to change relative to the cylinder. This additional degree of freedom allowed the forearm and cylinder to move out of the horizontal plane while the pointer remained in contact with the Plexiglas®. Ten-

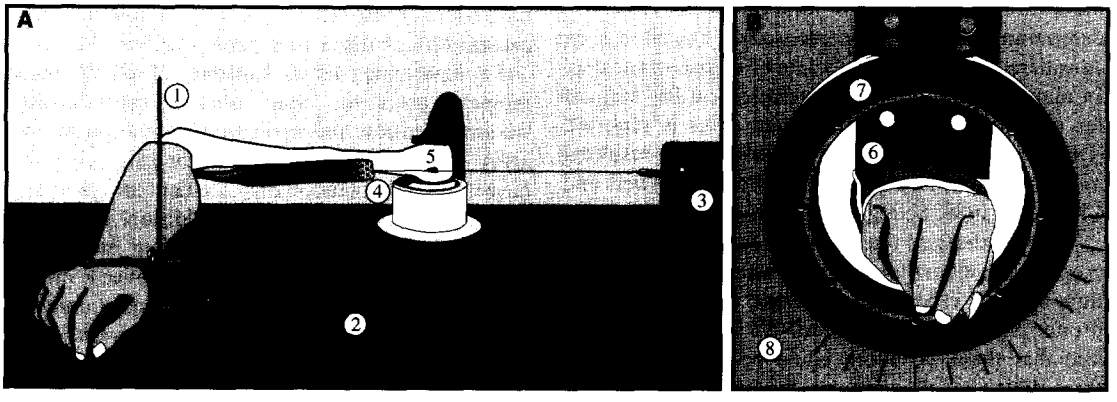

Fig. 1. (A). Experimental setup to measure tendon displacement with elbow flexion/extension. The pointer attached to the wrist (1) was aligned with etchings in the Plexiglas® surface at 5° increments (2). In this figure, the long head of the biceps is attached to the position transducer (3) via a wire. For the biceps, the wire was attached to a nylon mesh sewn to the muscle belly (4) and was routed through the intertubercular sulcus (5), to constrain the biceps to follow its anatomical path. The medial epicondyle of the humerus was mounted at the center of the goniometer (not shown). (B). Mounting of the specimen to measure tendon displacement with forearm pronation/supination (attachment of muscle to position transducer is similar to Fig. 1A). A fiberglass cast was placed on the wrist and an aluminum plate (6) was attached to the volar surface of the hand. The aluminum plate was bolted to the dial of the goniometer (7) so that the hand rested in the center of the circular ring. Angle measurements were made by aligning the arrow on the dial with etchings on the surface of the mounting device (8).

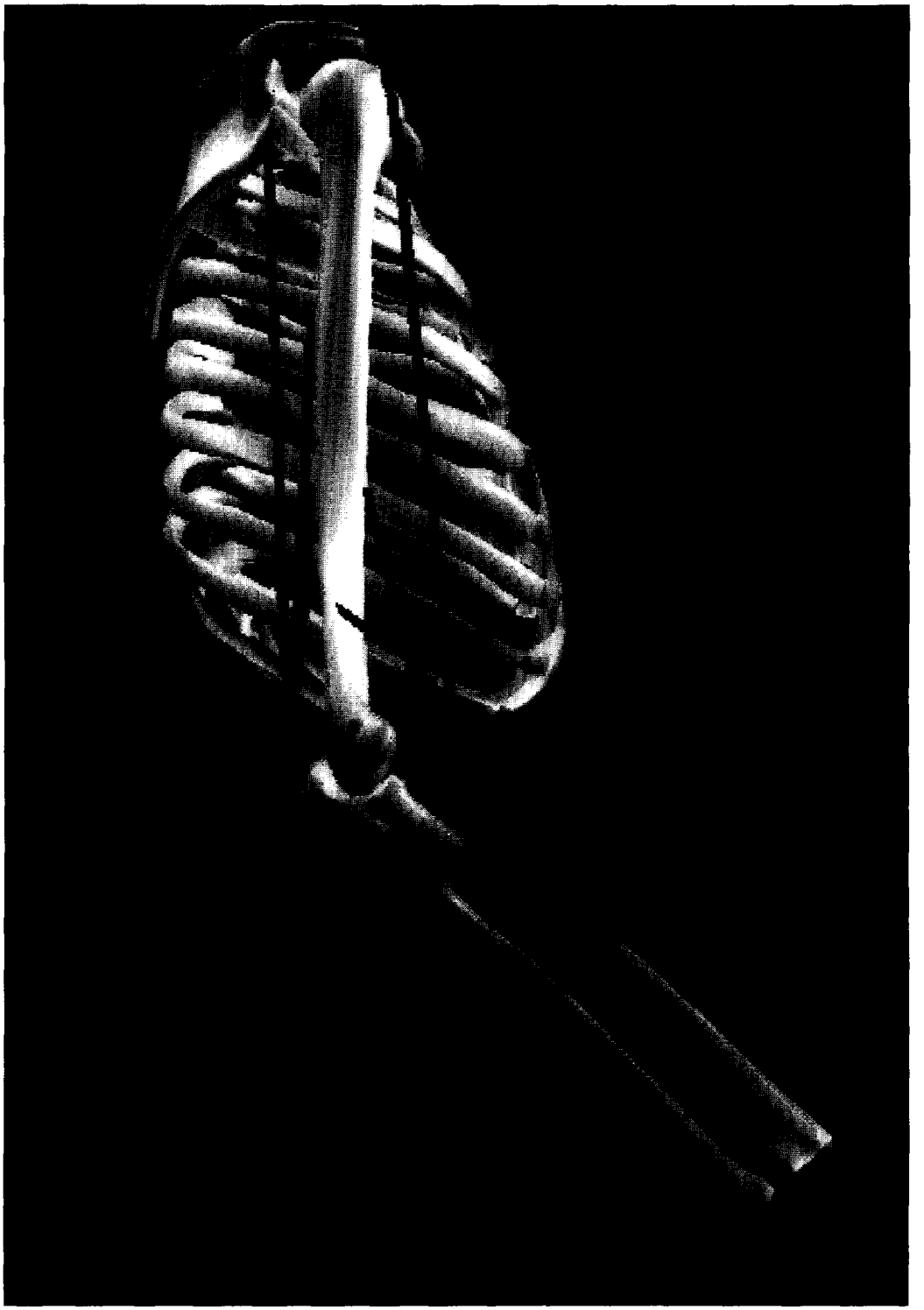

Fig. 2. Three-dimensional musculoskeletal geometry used to calculate moment arms. Muscles are modeled as a series of line segments. In addition to attachment sites on the bone, intermediate points are defined to constrain the path of the muscles that wrap around a bone or are constrained by retinacula. The number of points used to define a muscle path can vary with joint position.

don displacement vs elbow flexion angle was collected for three distinct forearm positions: the maximum pronated position for each specimen, mid-pronation/supination (neutral), and the maximum supinated position for each specimen.

Tendon displacement vs pronation/supination angle was collected at approximately 90° elbow flexion for each of the muscles studied. In addition, tendon displacement vs pronation/supination was measured with the elbow flexed 45° for the biceps. A fiberglass cast was placed on the wrist and an aluminum plate was attached to the volar surface of the hand. The aluminum plate was bolted to a goniometer so that the hand rested in the center of a rotating circle (Fig. 1B). The forearm position could be altered by rotating the dial of the goniometer.

A data set for a muscle in a particular protocol (e.g. the biceps flexion/extension protocol with the forearm in neutral) consisted of 7–12 trials. For each trial, the voltage of the length transducer was recorded at 5° increments in the flexion/extension protocol, or 10° increments in the pronation/supination protocol. Voltage was converted to length using the specifications of the position transducer given by the manufacturer. A fourth-order polynomial was fit to each of the flexion/extension data sets with a least-squares fit. The pronation/supination data were fit with a third-order polynomial. The analytical derivative of the polynomial fit was multiplied by -1 to determine the moment arm for the muscle and to maintain the convention of flexion and pronation as positive, extension and supination as negative. The polynomial fit was chosen because it effectively smoothed noise evident in the numerical derivatives of the tendon displacement data while other fitting methods, such as cubic and quintic splines, did not.

A computer model of the elbow joint and its surrounding musculature was developed using the musculoskeletal modeling software described by Delp *et al.* (1990). A musculoskeletal model is implemented in this system by specifying the geometry of the bones, kinematics of the joints, and lines of action of the muscles (Fig. 2).

The bones are defined by polyhedra that describe the bone surfaces. The computer model includes three-dimensional representations of the rib cage, scapula, clavicle, humerus, ulna, and radius which were obtained from Viewpoint Datasets (Orem, UT). Each of the bones has a reference frame in which the vertices of each polyhedra are expressed. The dimensions of the bones for the model are slightly larger than the bones from the female specimen, and smaller than the bones from the male specimen. In essence, this study contains three specimens, the two anatomical specimens and a 'simulated specimen', the computer model.

The elbow joint is defined by a homogeneous transformation from the humeral reference frame to the ulnar reference frame. Elbow flexion/extension is represented as a uniaxial hinge joint with its axis passing through the centers of the capitulum and the trochlear sulcus (London, 1981), Elbow flexion is modeled from full extension (defined here as 0° flexion) to 130° flexion. Forearm rotation is defined by a homogeneous transformation from the ulnar reference frame to the radial reference frame. During pronation and supination, the ulna remains stationary while the radius rotates about an axis that passes through the centers of the radial head and the distal ulna. Forearm rotation is modeled from 90° supination to 70° pronation. If the shoulder is adducted and the elbow is flexed 90°, the neutral forearm position (0° pronation/supination) is the position where the plane of the palm of the hand lies in the sagittal plane.

Muscle–tendon paths were defined based on the anatomical landmarks of the three-dimensional bone models. The long and short heads of the biceps, the brachialis, the brachioradialis, the pronator teres, and the long, medial, and lateral heads of the triceps are each modeled as a series of points connected by line segments. In addition to the origin and insertion points, intermediate 'via points' and 'wrapping points' were defined to model the path of the muscles that are constrained by retinacula or wrap around a bone, respectively. Because the muscle path varies with joint position, the number of points used to define a muscle path can vary with joint angle. For example, the tendon of the triceps wraps over the olecranon process of the ulna when the elbow is flexed more than 40°, but not when the elbow is extended. Thus, wrapping points are introduced at elbow flexion angles greater than 40° so that the triceps tendon wraps over the bone, rather than passing through the bone, in that range of motion. Moment arms were computed as the partial derivative of the muscle–tendon length, ∂l, with respect to joint angle, $\partial \phi$ (An *et al.*, 1984b; Storace and Wolf, 1979), that is

$$ma = \partial l / \partial \phi. \tag{1}$$

This is consistent with the method used to estimate moment arms in the anatomical study.

To assess the shapes of the moment arm vs joint angle curves quantitatively, the mean was removed from the flexion/extension moment arm curves and intraclass correlation coefficients (ICC) were calculated at 5° intervals between the curves for (1) the male and female specimens, (2) the male specimen and the computer model, and (3) the female specimen and the computer model.

RESULTS

Trial to trial variation in the tendon displacement data was minimal (Fig. 3), as is demonstrated by standard deviations on the order of 0.1 mm. The R^2 values of the polynomial fits to the tendon displacement data were greater than 0.995 in every protocol, indicating that the polynomial curves are good representations of the tendon excursion vs joint angle data.

Flexion moment arms calculated with the model and from the anatomical experiments show sizable

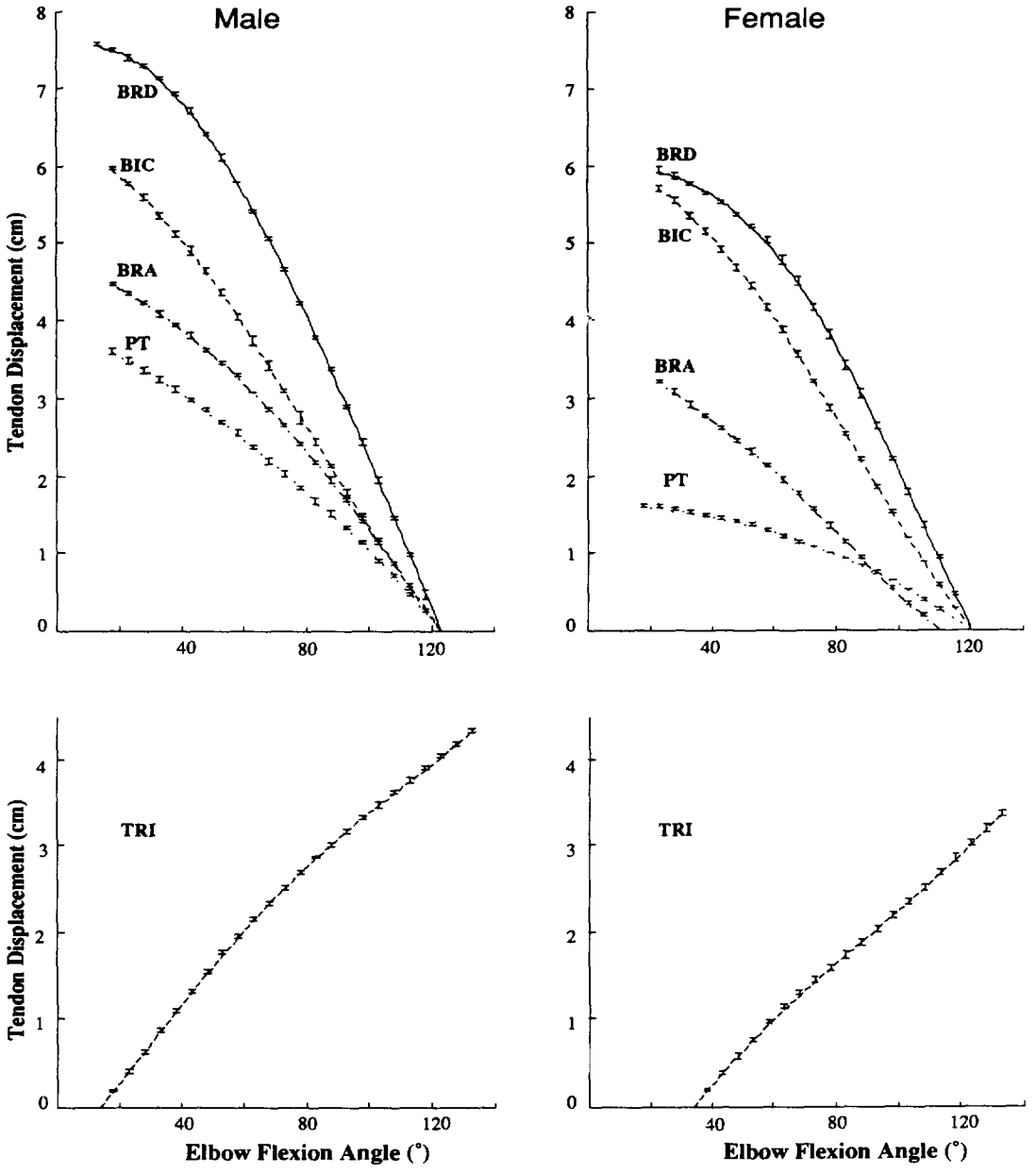

Fig. 3. Fourth-order polynomial fit to the tendon displacement vs joint angle data for the flexion/extension protocol with the forearm in neutral. The error bars shown are ± one standard deviation and were calculated from at least 7 trials for each muscle. The R^2 values of the polynomial fit were greater than 0.995 in every protocol.

variations with elbow flexion angle (Fig. 4). The anatomical data indicate that the moment arms of the brachioradialis, biceps, brachialis, and pronator teres increase with flexion, with the peak flexion moment arms occurring at greater than 75° of elbow flexion. The model estimates the moment arms of the major elbow flexors (brachioradialis, biceps, brachialis) to peak between 100° and 120°, and the peak moment arm of the pronator teres to be at approximately 75°. Over a 95° angular range (25–120°), the difference between the peak moment arm and the minimum moment arm is substantial for each muscle (Table 2).

The peak brachioradialis moment arms calculated from the anatomical measurements and the model reach approximately 6 cm between 100 and 120° flexion. The intraclass correlation coefficients (ICC) were greater than 0.96 for all three pairs of curves (male/female, male/model, and female/model). However, the brachioradialis moment arms measured in the two anatomical specimens decrease more rapidly with extension than the moment arm calculated with the model. The wire used in the anatomical measurements did not accurately approximate the thickness of the muscle belly and probably underestimated the

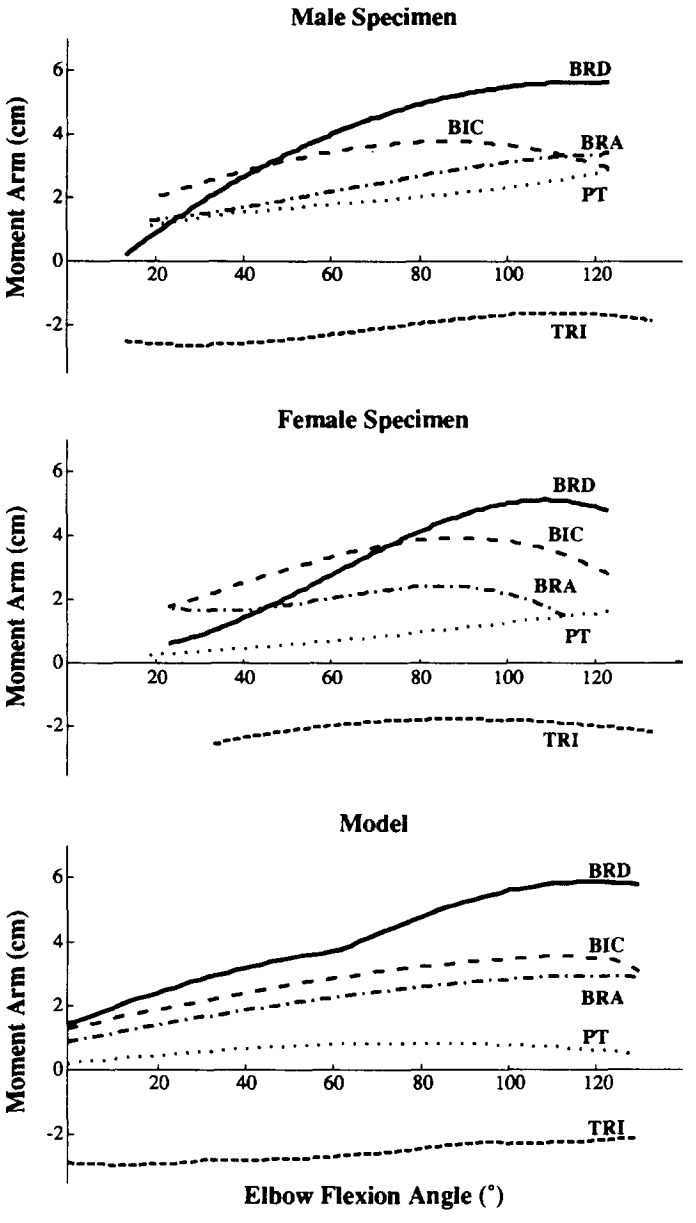

Fig. 4. Flexion/extension moment arms with the forearm in neutral for the brachioradialis (BRD), biceps (BIC), brachialis (BRA), pronator teres (PT), and triceps (TRI). Positive moment arms indicate flexion, negative moment arms indicate extension, 0° flexion angle is full extension. The derivatives of the polynomial fits of Fig. 3 were multiplied by −1 to maintain the convention of flexion moment arms being positive. Both the anatomical results and the model calculations show the brachioradialis has the largest peak flexion moment arm, followed by the biceps, the brachialis, and the pronator teres. In addition, all of the moment arms show substantial variation with elbow flexion angle.

Table 2. Percent difference* between the maximum and minimum flexion/extension moment arm from 25° to 120° elbow flexion

	Biceps	Brachialis	Brachioradialis	Pronator teres	Triceps
Male	40	58	75	54	38
Female	52	32†	86	79	29‡
Model	43	48	55	39	25

*The percent difference was calculated as the (maximum − minimum)/maximum.
†Angle range is 25–110° elbow flexion for the brachialis muscle in the female specimen.
‡Angle range is 35–120° elbow flexion for the triceps muscle in the female specimen.

brachioradialis moment arm near full extension, because the wire laid directly on the surface of the bone. Underestimation of the moment arm was avoided in the model by the addition of a wrapping point to the brachioradialis muscle path at 60° flexion; the wrapping point prevented the muscle path from moving into the humeral shaft near full extension. Without this anatomical constraint, the model moment arm calculation decreases to zero as rapidly as the anatomical curves. The discontinuity in the model moment arm curve at 60° flexion is due to the addition of the wrapping point to the muscle path.

The biceps moment arms calculated from the anatomical specimens peak at approximately 4.0 cm at 90° flexion compared to the moment arm calculated with the model which peaks at approximately 3.5 cm at 110° flexion. The ICCs for the biceps moment arm curves were greater than 0.8 for the male/model and female/model curves. The model calculation shown is the moment arm curve for the long head of the biceps. In the model, the moment arm curve for the short head of the biceps is identical to this curve because of the common insertion on the radius. The biceps also has an insertion on the ulna via the bicipital aponeurosis, which was not modeled and could affect the moment arm computed with the model (see Discussion).

The brachialis moment arm curve calculated from the tendon displacement data for the male specimen increases throughout the range of motion to a maximum of approximately 3 cm, as does the model curve (ICC > 0.99). The moment arm for the female specimen peaks at approximately 2.5 cm at 90° flexion, which differs from both the moment arms of the model and the male specimen (ICC < 0.7 for male/female and female/model). The difference between the anatomical moment arm curves may be due to an experimental difficulty caused by the large size of the brachialis in the female specimen, which did not translate well through the constraint simulating the retinaculum. The smaller brachialis muscle of the male specimen translated smoothly through the constraint. However, the wider and thicker muscle of the female specimen did not translate well between 100 and 120° flexion. This interfered with the muscle excursion and decreased the moment arm in addition to limiting the range of motion over which data could be collected.

The anatomical curves show strictly increasing moment arms for the pronator teres for both specimens, although the magnitude of the moment curve for the male specimen (1–3 cm) is approximately 1 cm larger than the curve for the female specimen (0–2 cm) for all elbow flexion angles. The model estimates the peak moment arm for the pronator teres to be approximately 1 cm at 75° flexion. The difference in the shapes of the moment arm curves is also indicated by ICCs < 0.35 for the male/model and the female/model curves.

The triceps extension moment arm curves calculated from the anatomical specimens have the largest values (≈ 2.5 cm) in the first 40° of flexion. The moment arm curve estimated with the model peaks (≈ 3.0 cm) in the first 25° of flexion, and decreases by 25% between 25 and 120° flexion. The model calculation shown is the moment arm curve calculated from the path of the medial head of the triceps. In the model, there are no substantial differences between this curve and the moment arm curves of the lateral and the long heads of the triceps because of the similar attachments on the ulna. The shape of the triceps moment arm curves differ for the anatomical specimens (ICCs < 0.8 for the male/female curves). The model moment arm curve has a 0.98 intraclass correlation coefficient with the male curve.

The magnitudes of the peak biceps supination moment arms of the anatomical specimens and the model are within 0.2 cm, but variation of the moment arms with joint angle is inconsistent (cf. Fig. 5, dashed curves). For the male specimen, the peak moment arm (≈ 1.3 cm) occurs near the neutral forearm position. The peak supination moment arm for the female specimen (≈ 1.1 cm) occurs while the forearm is supinated. The peak supination moment arm for the model (≈ 1.3 cm) occurs toward the most pronated forearm position.

The anatomical studies and the computer model show that the pronation moment arm peaks near the neutral forearm position for the pronator teres, but there are discrepancies in the peak magnitudes. The peak moment arm for the male specimen is approximately 0.5 cm; the peak for the female specimen is approximately 0.75 cm; and the peak pronation moment arm for the model is approximately 1.2 cm.

The brachioradialis pronation/supination moment arms estimated from the measurements of tendon excursion are small for the entire range of motion. Because the brachioradialis inserts on the distal radius, the casting of the forearm during the pronation /supination protocol may have interfered with the tendon excursion and underestimated the moment arm. The model calculation indicates that the brachioradialis has a pronation moment arm when the forearm is supinated and a supination moment arm when the forearm is pronated. Thus, this muscle tends to return the forearm to the neutral position. The model also indicates that the magnitude of the peak of the brachioradialis pronation/supination moment arm decreases from approximately 1.0 cm at 90° elbow flexion to approximately 4.0 mm at full elbow extension, while the shape remains consistent.

The pronation/supination moment arms for the brachialis and the triceps are not shown because both the anatomical curves and the model calculations indicate that the moment arms for these muscles are very near zero throughout the range of motion. This was expected because these two muscles insert on the ulna and are not involved in pronation/supination.

The flexion moment arm of biceps was affected by pronation/supination position more than any other muscle. The two specimens and the model show a larger peak flexion moment arm and a shift in the

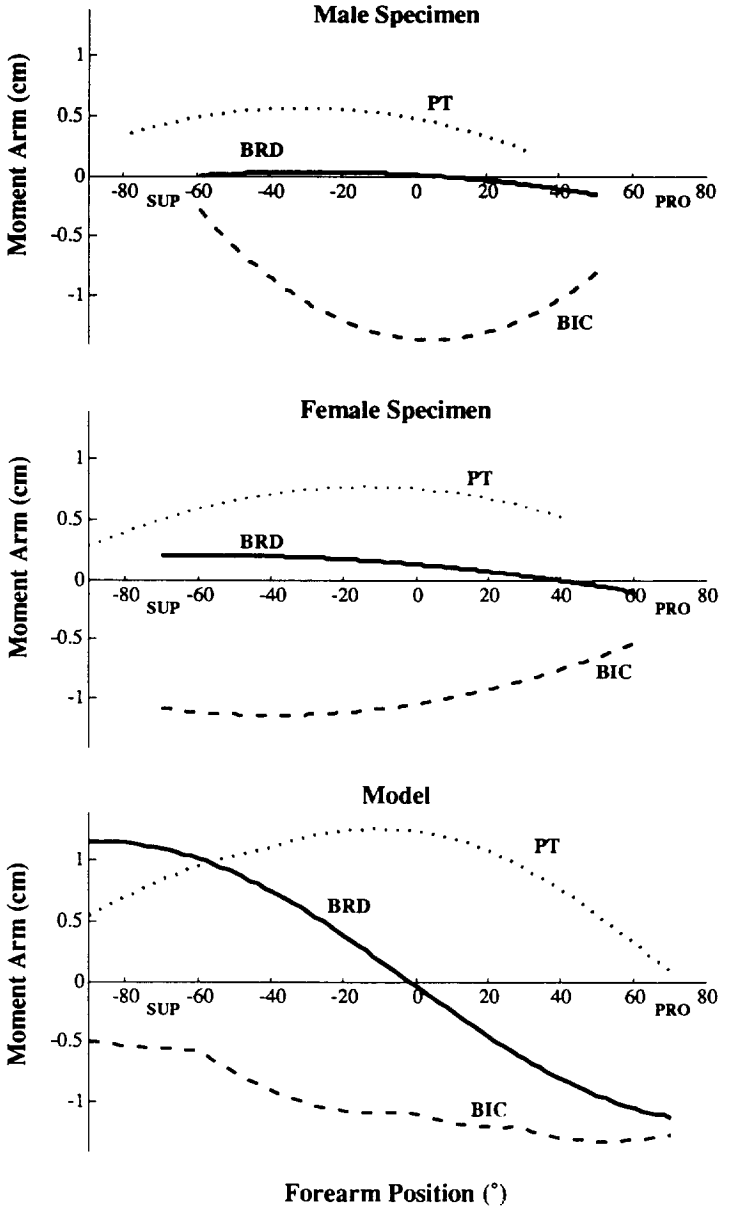

Fig. 5. Pronation/supination moment arms with the elbow flexed 85° for the pronator teres (PT), brachioradialis (BRD), and biceps (BIC). Negative angles and moment arms correspond to supination, positive angles and moment arms correspond to pronation. The neutral forearm position is 0°. Pronation/supination moment arm curves for the two anatomical specimens were different from each other and different from the computer model making it difficult to evaluate the variation of moment arm with forearm position.

location of the peak moment arm toward a more extended elbow position with the forearm in supination (Fig. 6). The peak moment arm of the male specimen increased 5 mm and occurred with approximately 20° more elbow extension when the forearm was fully supinated compared to when the forearm was fully pronated. For the female specimen, the peak moment arm increased approximately 7 mm and shifted 15° toward a more extended elbow position. The model calculates an increase in peak moment arm of approximately 5 mm that occurs with 10° more elbow extension. Although the model calculates the peak flexion moment arm at a more flexed elbow position that measured in the specimen, it does estimate the changes in the biceps flexion/extension moment arm due to forearm position.

The supination moment arm of the biceps decreases as the elbow is extended. For example, the moment arms are larger with the elbow flexed 85° than with the elbow flexed 45° in both the anatomical specimens and

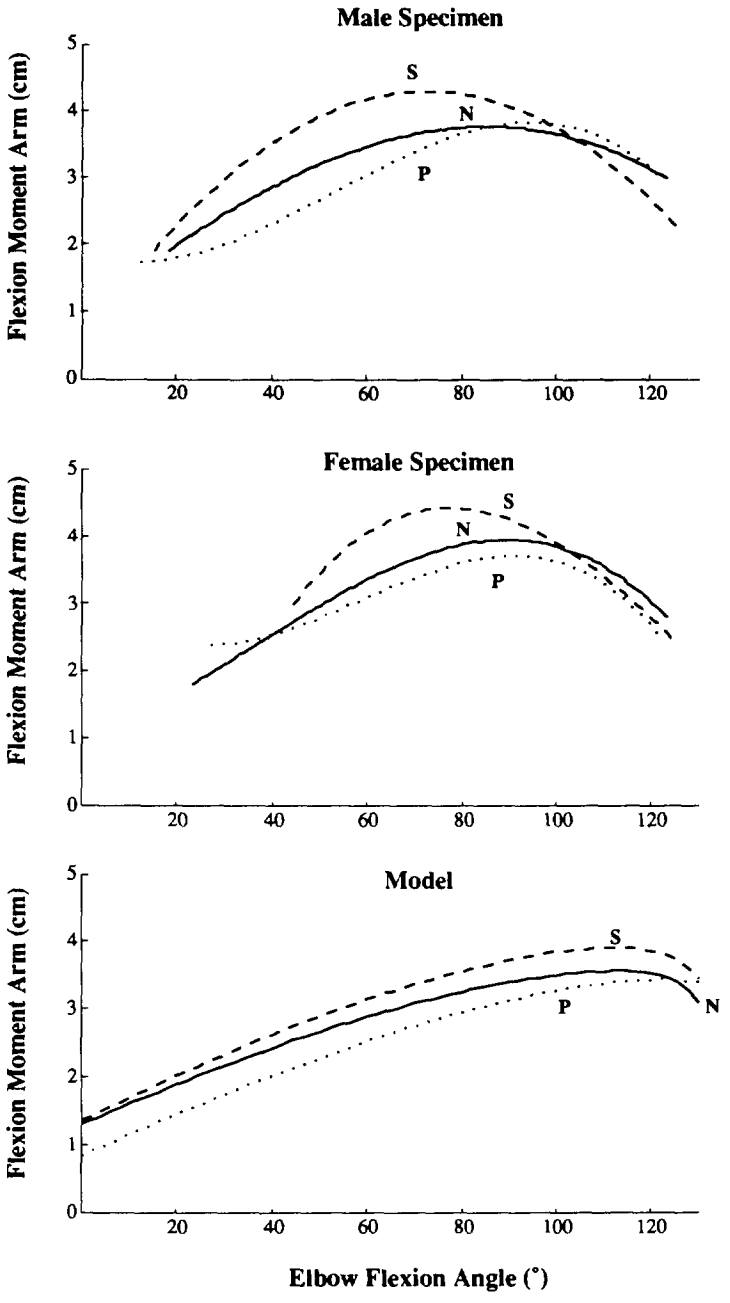

Fig. 6. Flexion moment arms for the biceps in three forearm positions: supinated (S), neutral (N), and pronated (P). The peak flexion moment arm increases from the pronated position to the supinated position. In addition, there is a shift in the location of the peak toward a more extended elbow position in both sets of anatomical data as well as the model.

the model calculations (Table 3). The peak supination moment arms decrease 48% for the male specimen, 34% for the female specimen, and 14% for the model when the elbow was extended from 85° flexion to 45° flexion.

DISCUSSION

The objective of this work was to determine if elbow muscle moment arms vary as a function of elbow flexion and forearm rotation and to determine if these variations could be represented in a three-dimensional computer model. The experimental results and the computer model showed that elbow flexion moment arms increase substantially with elbow flexion. We found that the pronation/supination angle can affect elbow flexion moment arms and the elbow flexion angle can affect pronation/supination moment arms. Specifically, the biceps flexion moment arm peaks in a

Table 3. Peak biceps supination moment arms at two flexion angles

	85° flexion	45° flexion
Male specimen	1.36	0.70
Female specimen	1.13	0.75
Model	1.32	1.14

Moment arm values are in cm.

more extended elbow position and has a larger peak when the forearm is supinated. In addition, the peak biceps supination moment arm decreases as the elbow is extended. These results emphasize the importance of considering limb position when estimating muscle moment arms about the elbow.

Before comparing our results with previous investigations, the effects of several assumptions and limitations of this study should be considered. In the experiments, the preparation of the muscles, the measurements of elbow angle and forearm position, and the data analysis method are potential sources of error. We have confidence in our anatomical moment arm estimates for a number of reasons. First, although the tendon excursion method requires dissecting the musculature and replacing portions of muscles with a wire, important anatomical constraints were maintained to ensure that each muscle translated along a reasonable approximation of its line of action. Second, the small standard deviations of the tendon displacement data illustrate that the measurement of elbow angle and forearm position was repeatable. Finally, because the polynomial fits of the tendon excursion data are excellent, the derivatives of the fits are good approximations of the muscle moment arms.

In the computer model, there are limitations caused by approximating muscle paths as a series of points connected by line segments. For example, broad muscle origins and insertions (i.e. brachialis) are approximated by a single point. Also, it is difficult to define muscle wrapping points that depend on more than one degree of freedom. These are common shortcomings of musculoskeletal models. In this study, the muscle paths were defined based on the anatomical landmarks of the digitized skeleton. Sensitivity studies were done to evaluate how sensitive muscle moment arms were to the locations of the attachment sites (see below). If our modeling system included the surface geometry of muscles that conformed to the bones and surrounding musculature based on surface interactions, it would provide a more accurate representation of muscle paths.

Finally, because anatomical measurements were made on two similarly sized specimens, we can make no conclusions about how moment arms vary among subjects of different sizes. Joint kinematics, the dimensions of the bones, and the relative shapes and cross-sectional areas of the muscles that surround the elbow all affect muscle moment arms. A detailed anatomical study that measures moment arms and quantifies relevant anatomical parameters of many differently sized specimens would be necessary to understand how these anatomical features affect the shapes and magnitudes of muscle moment arm curves. Even with this limitation, however, the current study presents a more comprehensive analysis of moment arms at the elbow joint than what is currently found in the literature.

The variations in muscle moment arms estimated by other elbow models (Amis *et al.*, 1979; Van Zuylen *et al.*, 1988; Wilkie, 1959; Winters and Kleweno, 1993) have not been quantitatively compared to anatomical measurements, since only a limited number of data points were previously available (An *et al.*, 1981, 1984a; Crowninshield and Brand, 1981). While the brachialis and triceps moment arms show reasonable agreement across studies, there are large difference for other muscles (Fig. 7). In particular, the brachioradialis peak flexion moment arm ranges from 4.0 to 8.0 cm, and the biceps peak ranges from 3.5 to 5.0 cm (Table 4). In addition, both the magnitude and shape of the pronator teres moment arm vary across studies.

In the development of the current model, we found that magnitudes and shapes of muscle moment arms could be substantially affected by the model of the muscle path. For example, the magnitude of the brachioradialis flexion moment arm is sensitive to the location of the attachment on the humerus. If the origin point is moved superiorly 1.5–2.0 cm on our computer model, it estimates peak magnitudes between 7.4 and 8.0 cm. This is the range that other elbow models estimate for the brachioradialis moment arm (Amis *et al.*, 1979; Van Zuylen *et al.*, 1988; Winters and Kleweno, 1993). However, the computer graphics display of the muscle paths raises questions to the accuracy of this representation. Specifically, the muscle path 'bow-strings' unrealistically away from the bone surfaces when the origin point is moved superiorly. Thus, although it is possible to match the estimations made by other models, an 8 cm brachioradialis flexion moment arm is too large for the size of the model developed in this study and is inconsistent with our anatomical results.

Similarly, other elbow models (Amis *et al.*, 1979; Van Zuylen *et al.*, 1988; Wilkie, 1959; Winters and Kleweno, 1993) estimate peak magnitudes for the biceps flexion moment arm that are comparable to each other but larger than the magnitude of the current model. It is difficult to resolve magnitude discrepancies with other models because no anthropometric data are reported in any of the studies, and the size of the limb could be a determining factor in moment arm magnitude. The close correspondence between the biceps moment arm computed with the model and the moment arms measured in the current study suggest that the magnitude of the biceps flexion moment arm is appropriate for the size of the current model. However, the issue of how the magnitude of

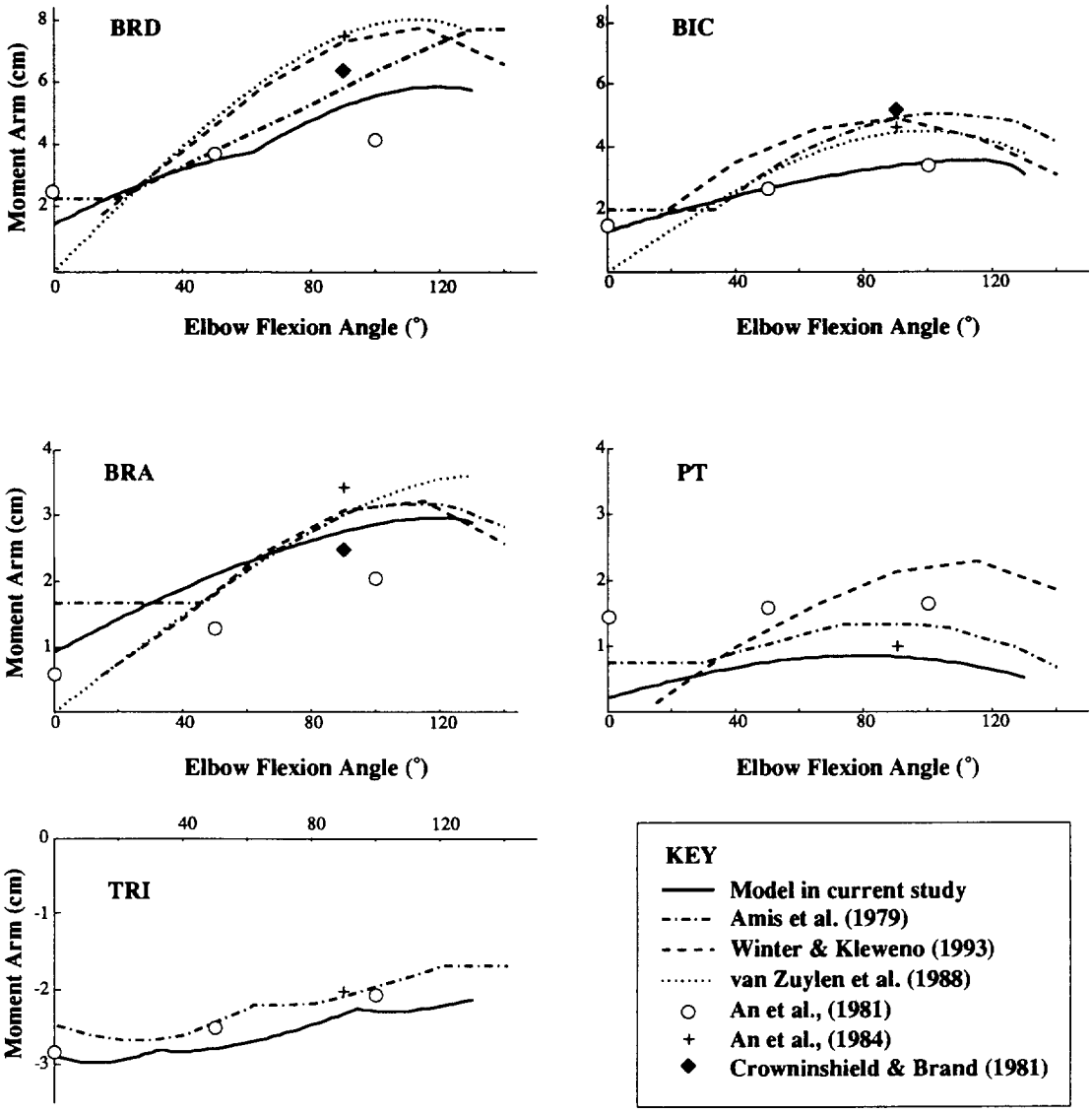

Fig. 7. Flexion/extension moment arms reported in the literature compared to the computer model estimations from this study. The data from An *et al.* (1981) are the moment arms measurements reported for the forearm in neutral. Amis *et al.* (1979) calculated moment arm curves based on the muscle paths of a specimen with the forearm pronated 30°. The model estimations from the current study are shown for the neutral forearm position. There are large differences in the shapes and magnitudes of elbow muscle moment arms reported in previous studies.

Table 4. Magnitude and angle ranges for the peak flexion/extension moment arms at the elbow joint (neutral forearm)

	Peak magnitude (cm)	Elbow angle of peaks (degrees)
Brachioradialis	4.0–8.0	> 105
Biceps	3.5–5.0	> 80
Brachialis	2.0–3.5	> 105
Pronator teres	1.0–3.0	> 75
Triceps	3.5–2.5	0–40

Data compiled from: Amis *et al.* (1979), Winter and Kleweno (1993), Van Zuylen *et al.* (1988), An *et al.* (1981, 1984), Crowninshield and Brand (1981), and the current study.

muscle moment arms vary among individuals of different sizes remains open.

In addition, the biceps flexion moment arm vs joint angle curve estimated by the current model peaks at approximately 10–20° greater flexion than the other curves. The biceps has two insertion points, one on the radius and one on the ulna via the bicipital aponeurosis. Our model of the biceps muscle path only represents the insertion point on the radius. Although the biceps moment arm calculated with the model is not sensitive to small shifts in the location of the insertion point on the radius, if the muscle path is modeled to attach to the ulna, the moment arm peaks

toward a more extended elbow position. However, with the insertion at the ulna, the magnitude of the flexion moment arm of the model decreases substantially and the supination moment arm of the biceps cannot be estimated. In order to maintain the most accurate representation of the muscle path for both flexion/extension and pronation/supination, we modeled the biceps insertion on the radius.

Finally, the high degree of variability in the pronator teres flexion moment arm in both the anatomical and modeling studies indicate the need for further examination of this muscle. Analysis of our model revealed that the moment arm is extremely sensitive to the location of the pronator teres attachment point on the medial epicondyle of the humerus. Shifting the pronator teres origin 2–4 mm in either the anterior–posterior or the superior–inferior directions has substantial effects on the shape and magnitude of the flexion moment arm. The sensitivity of the model calculation may be due to the proximity of the muscle origin to the axis of rotation for elbow flexion. This sensitivity probably causes the variability seen across studies.

The changes in musculoskeletal geometry that occur with pronation/supination are more complex than with flexion/extension. The wrapping of the muscles around the radius with pronation/supination is difficult to model and the small length changes that occur with pronation/supination make it difficult to measure pronation/supination moment arms. The estimations with our computer model accurately predict the functional roles of the pronator teres, biceps, and brachioradialis, but the exact shapes and magnitudes of the moment arm vs joint angle curves remain unclear. Previous studies have provided only limited information on pronation/supination moment arms. An *et al.* (1981, 1984a) report a few, discrete anatomical measurements of pronation/supination in different limb configurations. Winters and Kleweno (1993) had difficulty estimating pronation/supination moment arms and needed to scale model estimates of muscle moment arms upward by 33% to represent experimental measurements of pronation/supination moments accurately. The sparsity of data on pronation/supination moment arms in the literature, together with the variability seen in the results from the current study, indicate the need for further research in this area.

This study quantifies the changes that occur in the biceps flexion moment arm as a result of different forearm positions, as well as the decrease in the supination moment arm that occurs when the elbow is extended. These results emphasize the need to consider the position of the elbow and forearm when estimating elbow muscle moment arms. This point is evident in the flexion/extension moment arms for each of the muscles studied. In general, an average moment arm, or a measurement of moment arm at only one limb position, will not provide an adequate estimate of muscle moment arms for the entire range of motion. Because muscle moment arms have a profound effect on estimations of total joint moment, it is essential to account for variations with joint motion.

Acknowledgements—This work was supported by NIH R29 AR40408 and a grant from the Baxter Foundation. We would like to thank Lynette Hoppe for assistance with the illustrations and Paul Trpkovksi and Abraham Komattu for their assistance in this project.

REFERENCES

Amis, A. A., Dowson, D. and Wright, V. (1979) Muscle strengths and musculoskeletal geometry of the upper limb. *Engng Med.* **8,** 41–48.

An, K. N., Hui, F. C., Morrey, B. F., Linscheid, R. L. and Chao, E. Y. (1981) Muscles across the elbow joint: a biomechanical analysis. *J. Biomechanics* **14,** 659–669.

An, K. N., Kwak, B. M. and Chao, E. Y. (1984a) Determination of muscle and joint forces: a new technique to solve the indeterminate problem. *J. biomech. Engng* **106,** 364–367.

An, K. N. and Morrey, B. F. (1985) Biomechanics of the elbow, In *The Elbow and Its Disorders*, pp. 73–91. W. B. Saunders, Philadelphia.

An, K. N., Takahashi, K., Harrigan, T. P. and Chao, E. Y. (1984b) Determination of muscle orientations and moment arms. *J. biomech. Engng* **106,** 280–282.

Caldwell, G. E. and Chapman, A. E. (1989) Applied muscle modelling. Implementation of muscle-specific models. *Comput. Biol. Med* **19,** 417–434.

Crowninshield, R. D. and Brand, R. A. (1981) A physiologically based criterion of muscle force prediction in locomotion. *J. Biomechanics* **14,** 793–801.

Delp, S. L., Loan, J. P., Hoy, M. G., Zajac, F. E., Topp, E. L. and Rosen, J. M. (1990) An interactive graphics-based model of the lower extremity to study orthopedic procedures. *IEEE Trans. Biomed. Engng* **37,** 757–767.

Dul, J., Townsend, M. A., Shiavi, R. and Johnson, G. E. (1984) Muscular synergism—I. On criteria for load sharing between synergistic muscles. *J. Biomechanics* **17,** 663–673.

Edgerton, V. R., Apor, P. and Roy, R. R. (1990) Specific tension of human elbow flexor muscles. *Acta Physiol.* Hungarica **75,** 205–216.

Herzog, W. (1992) Sensitivity of muscle force estimation to changes in muscle input parameters using nonlinear optimization. *J. biomech. Engng* **114,** 267–268.

London, J. T. (1981) Kinematics of the elbow. *J. Bone Jt Surg.* **63A,** 529–535.

Murray, W. M., Delp, S. L. and Buchanan, T. S. (1992) Development of a graphics-based model of the human elbow: moment arm calculation issues. *Proc. NACOB II: The Second North American Congress on Biomechanics*, pp. 439–440.

Seireg, A. and Arvikar, R. J. (1973) A mathematical model for evaluation of forces in lower extremeties of the musculoskeletal system. *J. Biomechanics* **6,** 313–326.

Storace, A. and Wolf, B. (1979) Fundamental analysis of the role of the finger tendons. *J. Biomechanics* **12,** 575–578.

Van Zuylen, E. J., van Velzen, A. and Denier van der Gon, J. J. (1988) A biomechanical model for flexion torques of human arm muscles as a function of elbow angle. *J. Biomechanics* **21,** 183–190.

Wilkie, D. R. (1959) The relation between force and velocity in human muscle. *J. Physiol.* **110,** 249–280.

Winters, J. M. and Kleweno, D. G. (1993) Effect of initial upper-limb alignment on muscle contributions to isometric strength curves. *J. Biomechanics* **26,** 143–153.